Scientific Research Publishing

Journal of Materials Science and Chemical Engineering, 2026, 14(7), 10-28
https://www.scirp.org/journal/msce
ISSN Online: 2327-6053
ISSN Print: 2327-6045

Study and Characterization of a Composite Material Made from PVC Waste and Sand for Roofing Applications

Yaou Zakari[1], Layndé Tawé[1,2,3*], Bernard Dadi Gaga[4], Yannick Serge Evoung Nnengué[3], Ismael Figapka Pagoré[5], Noel Konai[1], Florent Biyeme[1]

[1]Department of Mechanical and Industrial Engineering, National Higher Polytechnic Institute, The University of Yaounde 1, Yaounde, Cameroon
[2]Department of Wood Construction, University of Institute of Wood Technology, The University of Yaounde I, Yaounde, Cameroon
[3]Department of Mechanical Engineering, Higher Teacher's Training College, The University of Ebolowa, Ebolowa, Cameroon
[4]Department of Wood Engineering, Higher Institute of Agriculture, Forestry, Water and Environment, The University of Bertoua, Bertoua, Cameroon
[5]Department of Basic and Applied Fundamental Science, Higher Institute of Agriculture, Forestry, Water and Environment, The University of Ebolowa, Ebolowa, Cameroon
Email: *tawecm5@yahoo.fr

How to cite this paper: Zakari, Y., Tawé, L., Gaga, B.D., Nnengué, Y.S.E., Pagoré, I.F., Konai, N. and Biyeme, F. (2026) Study and Characterization of a Composite Material Made from PVC Waste and Sand for Roofing Applications. *Journal of Materials Science and Chemical Engineering*, **14**, 10-28.
https://doi.org/10.4236/msce.2026.147002

Received: April 8, 2026
Accepted: July 24, 2026
Published: July 27, 2026

Abstract

This research deals with the valorization of polyvinyl chloride (PVC) waste and river sand for producing roof tiles. This study is based on an experimental analysis of roof tiles produced with varying proportions of recycled PVC and river sand: 10%, 20%, 30%, 40%, 50%, 60%, 70%, 80%, 90% and 100%, corresponding to samples 1 through 10, respectively, of PVC combined with the corresponding percentage of fine river sand aggregate. The PVC waste was heated to 170˚C to ensure it did not lose its properties. Tests were performed to evaluate the material's physical and mechanical performance, including water absorption, density, moisture content, and flexural strength. The following results were obtained: First, the water absorption rate of the composite varies between 1.267% (Sample 10) and 2.881% (Sample 1), with a mean value of 1.913% and a standard deviation of 0.551%. Second, the density of the composite varies between 1.0086 g/cm^3 (Sample 10) and 1.1111 g/cm^3 (Sample 1), with a mean value of 1.055 g/cm^3 and a standard deviation of 0.034 g/cm^3. Third, the applied force at the ultimate tensile stress of the composite varies between 32.3 N for a displacement of 0.395 mm in sample 10 and 205.3 N for a displacement of 0.9245 mm in sample 8. Samples 6, 7, and 8 show good results for use as composite materials for roofing tiles, but Sample 8 is chosen as the best composite material in this study because of its low absorption rate and density, which make it light and flexible for roofing use. Sample 8 is also a good choice because of its high strength, which gives the composite roofing tile resistance to rupture and cracking, thereby making it durable.

Keywords

Physical Properties, Mechanical Properties, PVC Waste, Sand Composite, Roofing

1. Introduction

Composite materials in roof construction are distinguished by their versatility and superior performance, offering a unique combination of lightness and mechanical strength. Composed of reinforcing fibers embedded in a polymer matrix, these materials allow customized properties tailored to project-specific requirements [1]. A primary advantage of roofing composites is excellent weather resistance: unlike wood, which rots, or metal, which rusts, composites resist both, ensuring enhanced roof durability and significantly lower long-term maintenance costs [2] [3]. Additionally, their malleability permits complex shapes and innovative designs, expanding architectural possibilities. This formal flexibility, combined with light weight, facilitates installation and reduces structural constraints on the building [4]. The roof, fundamentally the uppermost covering of any building, provides protection from rain, snow, wind, heat, and sunlight. As a superstructural element, its performance depends on both roof type and material selection [5] [6]. Traditional roofing materials include clay, concrete, and metal; more recently, composite materials incorporating sand and plastic have emerged. Roofs are inherently susceptible to weather-induced effects and failures, the most visible being collapse, corrosion, and leakages, all fundamentally material-based defects [7] [8]. Carbon fiber-reinforced composites represent the elite of roofing materials in terms of strength-to-weight ratio [9] [10]. These fibers, known for aerospace applications, offer exceptional rigidity while remaining extremely lightweight. For large-span roofs or bold architectural structures, carbon composites enable designs unachievable with conventional materials. Although more expensive than fiberglass composites, carbon fiber roofs constitute a worthwhile investment where lightness is critical or for iconic buildings requiring exceptional structural performance. Their outstanding fatigue resistance further ensures increased structural longevity [11].

Beyond high-performance carbon fiber systems, the necessity of producing roofing tiles from plastic waste and sand cannot be overstated. The availability of waste plastics is assured: of the 8.3 billion metric tons of plastics ever produced, approximately 6.3 billion metric tons have become waste, including PVC, the second most-used plastic after polyethylene [5] [12] [13]. Alarmingly, only 8.5% of these 6.3 billion metric tons are recycled; the remaining 91% accumulates in landfills and water bodies, causing severe environmental pollution and land degradation

[1] [14] [15]. This context provides compelling motivation for developing plastic/sand composite roofing materials that simultaneously address construction needs and waste management challenges.

Several research projects have advanced this objective. Notably, Yakum's investigation of river sand with plastic as a matrix yielded promising results: water absorption rates ranged from 3.62% to 0.11% at saturation, flexural strength reached 200.5 daN/cm^2, impact resistance measured 123 J/mm^2, and maximum drilling time occurred at 80% sand content. These findings demonstrated the composite's excellent rigidity and weather resistance, supporting its viability as a roofing material [16] [17]. Complementary studies explored conventional binders such as cement combined with PVC, revealing that mechanical properties and density of mortar decreased with PVC powder incorporation [18]. Another significant contribution proposed and empirically validated a high-reflectivity evaporation (HRE) composite roof, which synergistically integrates a high-reflectivity coating with a porous evaporation layer to achieve year-round energy savings [19]. Thermal insulation represents another major advantage of composite roofing materials [20] [21]. Their low thermal conductivity effectively contributes to indoor temperature regulation, reducing both heating and air conditioning requirements. This property holds particular value in the contemporary context of pursuing building energy efficiency [22]. Composites thus address multiple performance criteria simultaneously: structural capacity, durability, design freedom, and thermal management.

However, a critical problem persists: roofing materials currently available on the market remain expensive and prone to corrosion. This fundamental limitation justifies the rationale behind the present study. The convergence of factors unsatisfactory performance of conventional materials, the environmental imperative to valorize plastic waste, promising mechanical results from preliminary composite formulations, and the thermal and structural advantages composites offer establishes a clear research direction. Developing cost-effective, corrosion-resistant composite roofing materials from waste plastic and sand responds to an urgent need spanning economic, environmental, and technical domains.

2. Materials and Methods

2.1. Materials

Plastic waste, primarily from window frames and vehicle interior trim, and sand were collected from municipal landfills and urban drainage systems, respectively, in the Central Region of Cameroon. After washing and drying, this waste was ground into flakes ranging in size from 2 to 5 mm. River sand, collected from the bed of the Sanaga River, is washed, dried, and then sieved to obtain a particle size of 1.25 mm or smaller. These characteristics directly influence the compactness of the mixture and the final properties of the composite. They are used here as raw materials to be mixed in varying proportions. **Figure 1(a)** shows PVC waste and **Figure 1(b)** shows river sand.

Figure 1. (a) PVC waste, (b) River sand.

Figure 2 below shows a shredder machine incorporated with a rotating cutting blade. The PVC wastes are fed into the machine through the hopper and the rotary blade inside the shredder and the plastic is cut into the required small flakes.

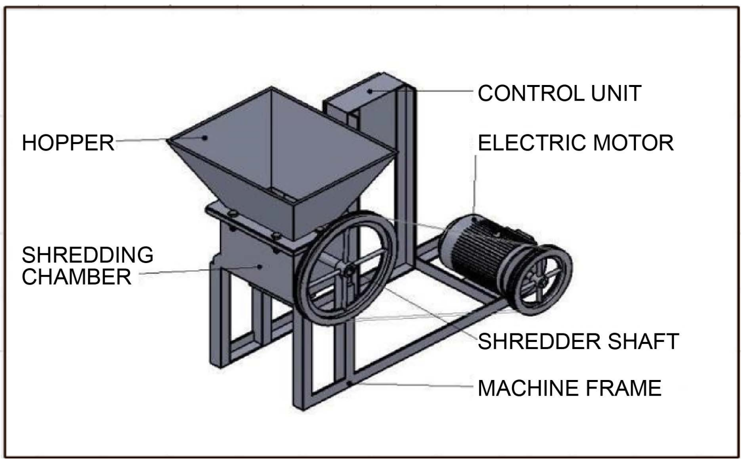

Figure 2. Plastics shredder machine modelling.

Figure 3(a) presents a furnace and Figure 3(b) a mold: A heating furnace is used to melt the shredded plastic flakes and then placed into a mold to form the specimens from the mixture of molten plastics flakes and sand.

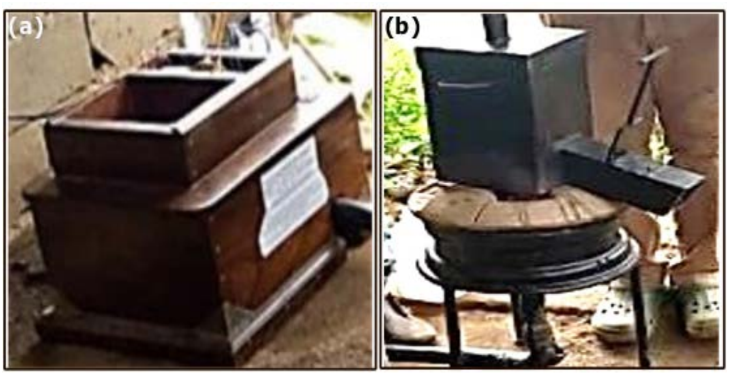

Figure 3. (a) Furnace, (b) Mold (no more than 1.5 cm deep).

Figure 4 below shows the specimen obtained for characterization. An electronic scale was used to measure the specimens before and after water absorption. After the measurement, an oven was used to dry the specimens, in order to drain water from it.

Figure 4. Samples of PVC waste/sand composite.

Figure 5 below shows a three-point bending machine used to carry out bending test. The equipment (bending machine) has a maximum force of 5 kN and a maximum crosshead speed of 500 mm/min. The test was performed in accordance with NF EN 312-2 (2014). The sample was placed on two supports. The specimens of the size 160 × 40 × 40 mm were tested for flexural strength. The deformation process was set up until failure occurred.

Figure 5. Three-point bending machine.

According to standard NF EN 490, the bending stress is calculated using the following formula:

$$\sigma_f = \frac{3FL}{2bh^2} \quad (1)$$

where;

F: maximum flexural load (N).

L: length of test sample (mm).
W: width of test sample (mm).
d: thickness of test sample (mm).

2.2. Methods

Considering that the right PVC waste is selected, washed, dried, and ground to smaller granulates to ease melting and the sand is washed, dried and sieved to obtain granulates of a maximum of 1.25 mm, measurement of the percentages by mass of plastic to sand were calculated and summarized in **Table 1** below.

Table 1. Summary of PVC and Sand ratios.

Samples	PVC (%)	Sand (%)	PVC:Sand ratio
1	10	90	10:90
2	20	80	20:80
3	30	70	30:70
4	40	60	40:60
5	50	50	50:50
6	60	40	60:40
7	70	30	70:30
8	80	20	80:20
9	90	10	90:10
10	100	0	100:0

2.2.1. Melt of Plastics

The oven is preheated to 170˚C ± 2˚C (temperature controlled by a thermocouple). PVC flakes are added in 50-g increments to a metal container. Heating continues for 15 minutes until a homogeneous, viscous paste is obtained.

2.2.2. Mixing and Molding

Continue stirring thoroughly until all the PVC scraps have melted and you have a smooth, viscous liquid. Keep mixing and heating until all lumps have disappeared and a smooth paste is formed, as lumps can compromise the material's strength. This can take up to 20 minutes [2] [23] [24]. Add the previously weighed amount of sand, stirring constantly until the desired mixture is achieved. Continue mixing so that the plastic, which acts as a binder, is thoroughly incorporated and has the appearance of gray cement. Prepare the mold, ensuring it is perfectly clean, with no plastic residue from previous castings. Quickly remove the mixture using a metal-handled shovel and pour it into the mold using a trowel. Pack the mixture into the mold so that no air pockets remain. The mixture is poured into a steel mold that has been pre-lubricated. Cooling takes place at room temperature (25˚C ± 2˚C) for 30 minutes before demolding.

2.2.3. Setting

Allow the hot mixture in the mold to set for a few minutes, repeatedly shaking the mold to perfectly fill the edges. Keep trying to lift the mold. When the mixture has hardened enough that the slab will not collapse, remove the mold. It should harden within 10 minutes. Repeat this procedure to produce the samples with different percentages of sand and PVC waste. Figure 6 below shows the flowchart of the processing of PVC waste and the sand samples used in the study.

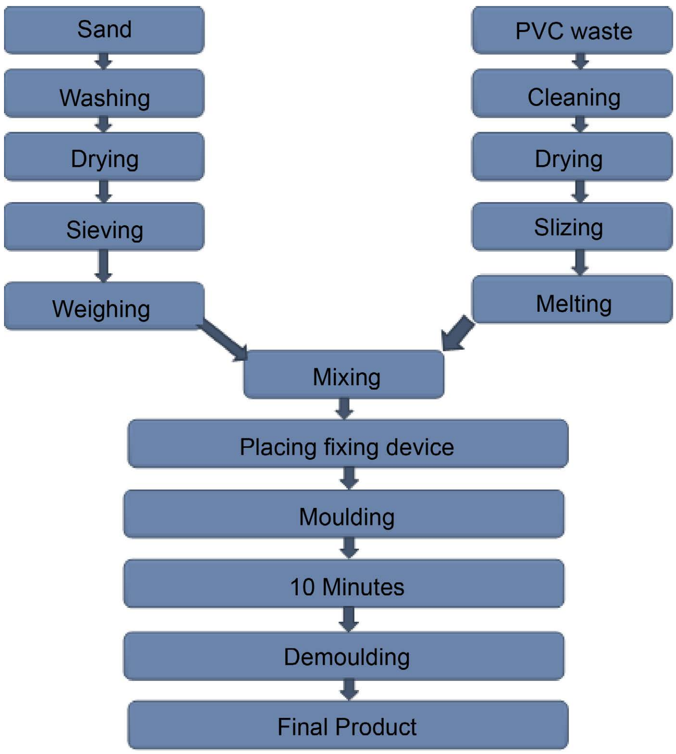

Figure 6. Flow chart of the manufacturing of PVC waste and the sand samples.

2.2.4. Determination of Absolute Density

To determine the absolute density, it is necessary to first know the parameters recorded in Table 2 below in order to apply the procedure of the international standards.

Table 2. Test parameters [3] [25].

Materials	Biofilms
Number of samples	10
PH of the water	7

Procedure

- Cut and mark the samples;
- Dry the samples in an oven at 60˚C until they are anhydrous;

- Weigh the sample and record its mass m_e;
- Fill the test bed with distilled water;
- Introduce the sample and record the volume of the sample V_e;

The absolute density is determined by the following formula:

$$\rho_{abs} = \frac{m_e}{V_e} \text{ in g/cm}^3 \quad (2)$$

where: m_e: mass of the sample; V_e: volume of the sample

For this physical test, we used 10 samples measuring 50 × 25 × 10 mm in accordance with ISO 1183-1, which specifies the immersion method for plastics.

After determining the densities as a function of the combinations of the composite material, we have summarized the results in Table 3 below.

Table 3. Statistical surveys of density.

Samples	PVC (%)	Sand (%)	Density (g/cm^3)	Standard deviation (g/cm^3)
1	10	90	1.1111	0.0341
2	20	80	1.1056	0.0337
3	30	70	1.0802	0.0329
4	40	60	1.0665	0.0325
5	50	50	1.0577	0.0322
6	60	40	1.0400	0.0317
7	70	30	1.0389	0.0316
8	80	20	1.0250	0.0312
9	90	10	1.0137	0.0309
10	100	0	1.0086	0.0307

2.2.5. Determination of Kinetics Absorption and Absorption Rates

Table 4 below summarizes the parameters used to determine the water absorption kinetics.

Table 4. Test parameters [26].

Test Parameters	Biofilms
Number of samples	10
PH of the water	7
Drying temperature	80˚C

A series of samples was taken from each of the composite plates to measure the kinetics of water absorption. To monitor water absorption in composites, a gravimeter is used. It consists of monitoring the mass evolution of the samples over time, measured at regular intervals over a total period of 5 days (120 h). At the time of the mass measurement, the samples (previously dehydrated in an oven and then immersed in a water bath) are removed and lightly wiped with an absorbent paper to eliminate the film of water on the surface. The samples are then weighed and re-immersed. A laboratory scale, accurate to 0.001 g, is used for these measurements, which are necessary to calculate the water absorption rate. For each formulation, we used 10 test specimens measuring 50 × 25 × 10 mm, in accordance with ASTM D570 for the water absorption of plastics.

Fick's model [27] [28]

After different immersion times, the water absorption characteristics of the composites are determined by the percentage by mass of water absorbed M_t at time *t*, and defined by the equation:

$$M_t = \frac{W_t - W_0}{W_0} \times 100(\%) \tag{3}$$

where W_0 is the mass of the unaged sample at $t = 0$ and W_t is the mass of the aged sample at time *t*. The diffusion coefficient D is determined by the following equation, in the case where the M_t values are less than 60% of the saturation value M_m [29] [30]:

$$D = \pi\left(\frac{k}{4M_m}\right)^2 \tag{4}$$

where k is the slope of the linear part of the curve $M_t = f\left(\sqrt{t}/h\right)$ and M_m is the maximum mass in water at equilibrium.

In addition, a correction factor is required to account for the fine dimensions of the specimens:

$$D_c = D\left(1 + \frac{h}{L} + \frac{h}{w}\right)^{-2} \tag{5}$$

where D_c is the corrected transverse diffusion coefficient, L and w are the length and width of the specimen, respectively. The test results are summarized in Table 5 below.

Table 5. Statistical records of the water absorption rate.

t (hours)	0	1	2	3	24	48	72	96	$\%A$	$\%A_{avg}$	σ
Sample 1	15.41	15.67	15.635	15.665	15.742	15.815	15.852	15.854	2.881	-	-
Sample 2	13.754	13.786	13.798	13.798	13.902	14.04	14.104	14.129	2.726	-	-
Sample 3	11.972	12.022	12.025	12.037	12.149	12.211	12.23	12.25	2.322	-	-
Sample 4	20.021	20.061	20.099	20.087	20.225	20.343	20.392	20.394	1.863	1.913	0.551
Sample 5	17.995	18.08	18.091	18.108	18.209	18.283	18.297	18.327	1.844	-	-
Sample 6	17.099	17.146	17.151	17.161	17.274	17.336	17.381	17.393	1.719	-	-
Sample 7	13.31	13.338	13.344	13.359	13.408	13.468	13.492	13.517	1.555	-	-
Sample 8	14.657	14.708	14.717	14.715	14.781	14.844	14.87	14.874	1.480	-	-
Sample 9	13.728	13.774	13.797	13.8	13.855	13.868	13.927	13.93	1.471	-	-
Sample 10	18.849	18.912	18.916	18.917	19	19.053	19.079	19.088	1.267	-	-

To validate the goodness-of-fit of the Fickian diffusion model, the coefficient of determination (R^2) was calculated for each formulation by linear regression of the experimental data M_t versus $\sqrt{t}/h$ over the initial linear region (where $M_t < 60\%$ of M_m). The R^2 values, ranging from 0.967 to 0.994, indicate excellent agreement between the experimental data and the Fickian model, confirming the diffusive nature of water absorption in these composites. The fitting curves and R^2 values are presented in Table 6.

Table 6. Statistical survey of absorption kinetics with R^2 goodness-of-fit values for the Fickian diffusion model.

Sample	M_t (%)	$\sqrt{t}/h$	k	D ($\times10^{-6}$ mm²/s)	D_c ($\times10^{-6}$ mm²/s)	R^2
Sample 1	0 → 2.881	0 → 0.816	4.0375	0.385	0.143	0.987
Sample 2	0 → 2.726	0 → 0.816	3.4483	0.313	0.116	0.982
Sample 3	0 → 2.322	0 → 0.816	3.5321	0.454	0.168	0.979
Sample 4	0 → 1.863	0 → 0.816	2.7113	0.415	0.154	0.991
Sample 5	0 → 1.844	0 → 0.816	4.3775	1.104	0.410	0.967
Sample 6	0 → 1.719	0 → 0.816	2.4569	0.400	0.149	0.994
Sample 7	0 → 1.555	0 → 0.816	1.8801	0.286	0.106	0.988
Sample 8	0 → 1.480	0 → 0.816	1.9882	0.353	0.131	0.985
Sample 9	0 → 1.471	0 → 0.816	2.0667	0.387	0.143	0.978
Sample 10	0 → 1.267	0 → 0.816	1.7924	0.392	0.145	0.996

2.2.6. Determination of Moisture Content NFB 51-004

The moisture content is determined on the basis of ten samples as shown in Table 7 below.

Table 7. Test parameters [31].

Materials	Biofilm
Numbers of samples	10

Procedure

- Cut and mark the samples;
- Weigh the sample and record m_0;
- Place the sample in an oven preheated to 80˚C for 10 minutes;
- Remove the sample, reweigh it and return it to the oven;
- Repeat the process until the successive variation between two measurements is less than 5% of the mass of the sample;
- We used dimensions of 50 × 25 × 10 mm in accordance with the standard for plastics regarding moisture content.

The moisture content is calculated by the formula

$$H(\%) = \frac{m_0 - m_f}{m_0} \times 100\% \tag{6}$$

m_0 : initial mass and m_f final mass, all in g.

After that, we summarized the results obtained in Table 8 below.

Table 8. Statistical humidity records.

t (minutes)	0	180	$\%H$	$\%H_{avg}$	σ
Sample 1	14.562	14.55	0.08240626	-	-
Sample 2	16.779	16.721	0.34567018	-	-
Sample 3	11.511	11.498	0.11293545	-	-
Sample 4	13.658	13.645	0.09518231	-	-
Sample 5	14.788	14.779	0.06086016	-	-
Sample 6	14.12	14.104	0.11331445	-	-
Sample 7	12.263	12.249	0.11416456	0.15234125	0.09752573
Sample 8	18.971	18.954	0.08961046	-	-
Sample 9	15.248	15.204	0.28856243	-	-
Sample 10	14.952	14.919	0.22070626	-	-

2.2.7. Determination of Tree Point Bending Test

The bending behavior of the material was determined using the LDW-1 universal mechanical testing machine of CeCaM (Characterization Center of Materials, Cameroon). This machine is computer-controlled. Its maximum force cell is 5 kN and the maximum crosshead speed is 500 mm/min. The test was performed in accordance with NF EN 312-2 (2014) [30].

The specimen was placed on two support platforms. Its deformation to failure was achieved using purling applied at an equal distance from the supports with a constant speed of 2 mm/min. The distance between the supports was taken to be 80 mm. During the experiments, the force applied by the purling F and the displacement of the beam were recorded. These data were used to obtain the force-displacement curves.

3. Results and Discussion

Table 9 below summarizes the statistics for the various properties studied. We have identified the minimum and maximum values for each sample, as well as the means and standard deviations for each property.

Table 9. Summary table of the statistics examined.

Properties	minimum	maximum	mean	Standard deviation
Water Absorption rate (%)	1.267 (S10)	2.881 (S1)	1.913	0.551
Density (%)	1.0086 (S10)	1.1111 (S1)	1.055	0.034
moisture content (%)	0.0608 (S5)	0.3456 (S2)	0.152	0.098
breaking strength (N)	32.3 (S10)	205.3 (S8)	88.7	-

3.1. Density Histogram

Results obtained from Table 2 have been summarized to obtain the graph of density distribution of the PVC waste and sand composite below (Figure 7).

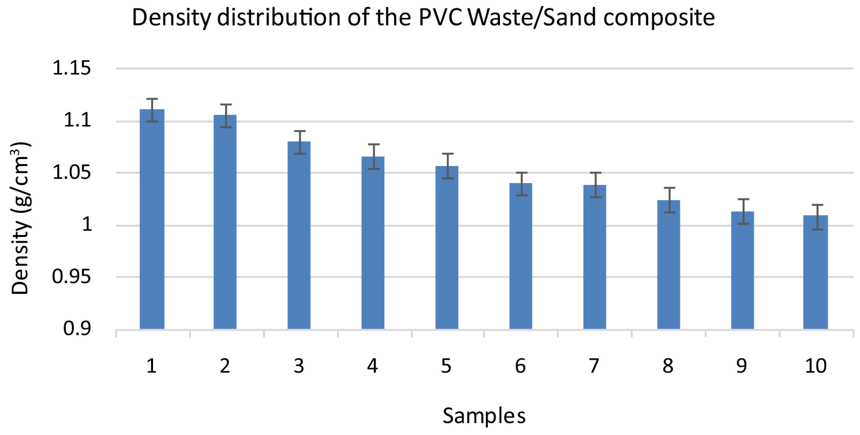

Figure 7. Density Histogram for PVC waste/sand composite density.

The density histogram for the PVC waste/sand composite (Figure 7) shows that the density varies between 1.0086 g/cm^3 (Sample 10, 100% PVC) and 1.1111 g/cm^3 (Sample 1, 10% PVC), with a mean value of 1.055 g/cm^3 and a standard deviation of 0.034 g/cm^3. The density decreases as the proportion of PVC increases, which is advantageous for roofing applications because lower density results in lighter tiles. These results are consistent with those obtained by G.O. Bamigboye in ref [32] and Mehdi Seghiri in ref [33], and comply with the NF EN 1304 standard.

3.2. Water Absorption Rate

Results obtained have been summarized to obtain the graph of absorption distribution of the PVC waste and sand composite below (Figure 8).

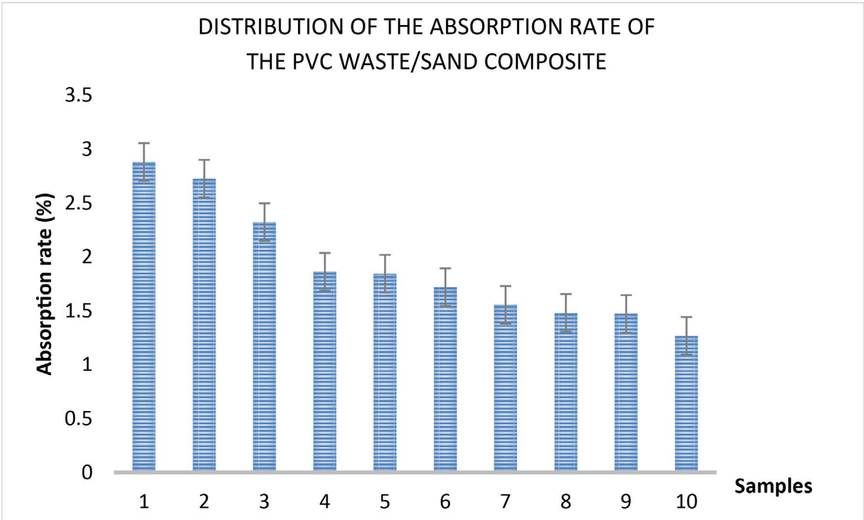

Figure 8. PVC waste /sand composite for water absorption rate.

The histogram of water absorption rates above shows the variation in water absorption rates for each sample. However, the tenth sample performs the best, as it absorbs less water than the others. The water absorption rate ranges from 1.267% (sample 10) to 2.881% (sample 1), with a mean value of 1.913% and a standard deviation of 0.551%. The absorption rate decreases as the PVC content increases, demonstrating the hydrophobic nature of the polymer matrix. These results are consistent with those obtained by G.O. Bamigboye in ref [33].

3.3. Water Absorption Kinetics

The fitting curves and R^2 values are presented in **Figure 9** below. The slope k of the linear portion of the curve $M_t = f\left(\sqrt{t}/h\right)$ was determined by linear regression for the first 24 hours ($M_t < 60\%$ of M_m). The diffusion coefficient D was calculated using Equation (4), then corrected using Equation (5). The obtained values are presented in **Table 6**. The goodness-of-fit of the Fickian diffusion model was validated by calculating the coefficient of determination (R^2) for each formulation.

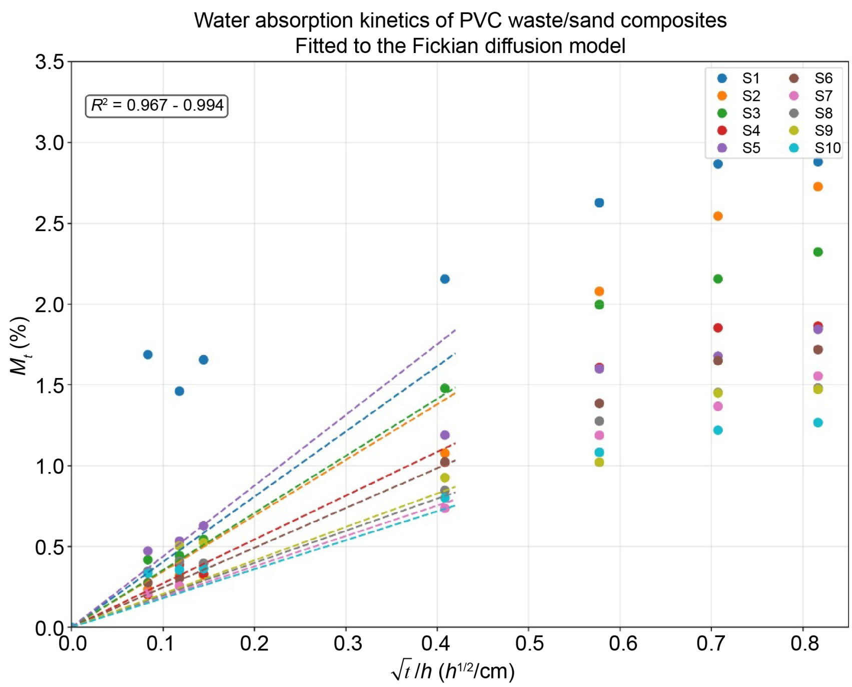

Figure 9. Water absorption kinetics of the PVC waste/sand composites.

The water absorption kinetics of the PVC waste/sand composites were investigated by monitoring the mass evolution of samples over a 96-hour immersion period. The R^2 values range from 0.967 (Sample 5) to 0.994 (Sample 6), with all values exceeding 0.96, demonstrating excellent agreement between the experimental data and the Fickian model. This confirms that water absorption in these composites follows Fickian diffusion behavior, characterized by a linear relationship between mass uptake and the square root of time divided by thickness during the initial stage. The corrected diffusion coefficients D_c range from 0.106 × 10^{-6} mm^2/s (Sample 7) to 0.410 × 10^{-6} mm^2/s (Sample 5). These relatively low values indicate that the material is hydrophobic [8] [16], making it an ideal candidate for roofing tile applications where water resistance is essential. The slight decrease in diffusion coefficients with increasing PVC content can be attributed to the hydrophobic nature of the polymer matrix, which reduces water ingress into the composite. The validation of the Fickian model with high R^2 values provides a reliable basis for predicting long-term water absorption behavior of these composites under service conditions. Since these values, measured over 96 hours, are relatively low, it can be concluded that the material is hydrophobic [8]. This makes it an ideal alternative for the manufacture of roof tiles that are moisture-resistant and durable.

3.4. Moisture Content Histogram

Figure 10 shows the moisture content of the composite, which varies between 0.0608% (Sample 5) and 0.3456% (Sample 2), with a mean value of 0.1523% and a standard deviation of 0.0975% (calculated from Table 8). These low values indicate that the composite is insensitive to humidity, as both constituent materials (sand and PVC) are also insensitive to moisture. Consequently, the effect of moisture on the degradation of the sand-reinforced PVC composite tiles will be minor, making this composite ideal for roofing applications.

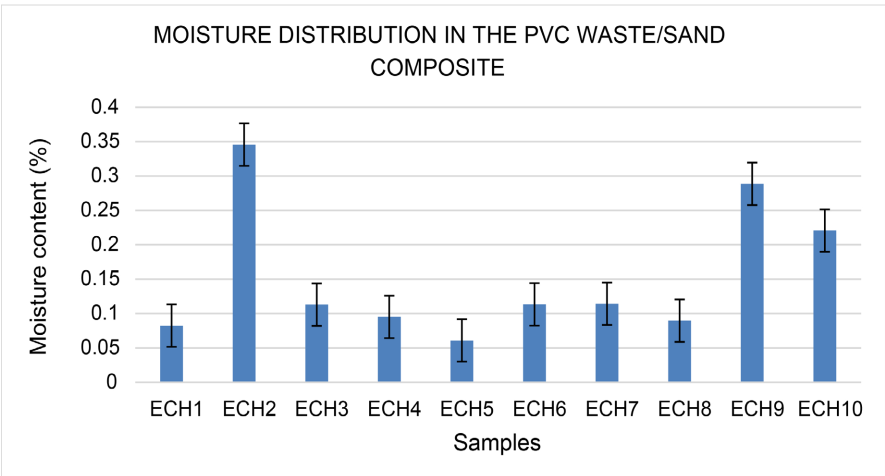

Figure 10. Moisture content chart.

3.5. Flexural Strength

Figure 11 shows the force-displacement curves obtained during three-point bending tests on the various PVC/sand composite specimens.

Figure 11 below shows the flexural strength of the composite. From the flexural graph below, the forces noted at the ultimate stress point vary between 32.3N for a displacement of 0.395 mm in sample 10, and 205.3N for a displacement of 0.9245 mm in sample 8. The average force for samples 1 to 10 to undergo failure should be 88.7N. It is important to note that, the higher the displacement of the material, the better its elasticity. As such, the material is void of brittleness. Therefore, the sample denoted 8 is the best choice for the composite roofing tiles even though it less dense and has a higher water absorption rate than sample 10. This is because sample 10 has a low strength or flexural strength than sample 8 and thus sample is brittle and vulnerable to crack and breakage.

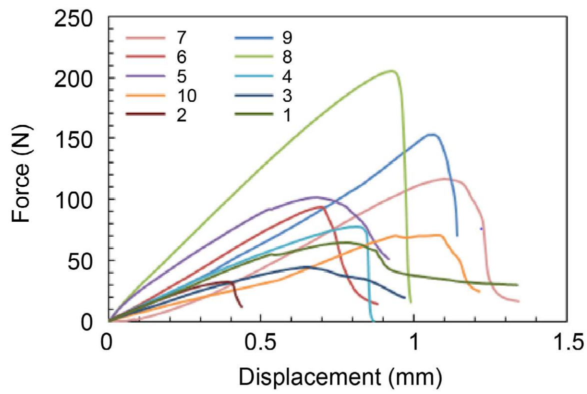

Figure 11. Force-displacement curve.

3.6. Bending Stress

The flexural stress (or rupture stress) was calculated from the maximum recorded force, using equation (1) presented in section 2-2-7. Figure 12 illustrates the evolution of flexural stress as a function of PVC content.

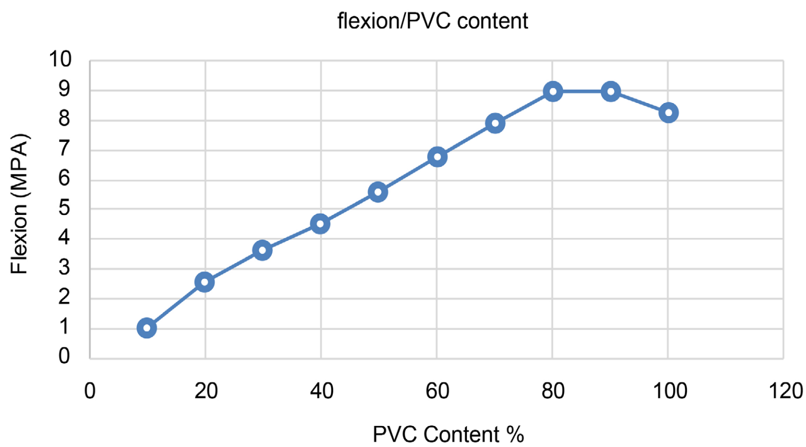

Figure 12. Bending strength curve as a function of plastic content.

This figure shows how flexural strength varies with plastic content. It demonstrates that flexural strength increases when the plastic content is between 10% and 80%. Specifically, for plastic contents ranging from 80% to 100%, flexural strength increases by 8 to 9 MPa. The increase in strength for plastic contents of 80 to 100% could be explained by the fact that the mixture contains a sufficient amount of plastic to bind or coat the sand grains. Flexural strength is low when the plastic content is between 10 and 30%. For these contents, the strength drops from 1 to 3.5 MPa. Above 30% plastic, the strength increases because the amount of plastic in the mixture is high. Indeed, the more plastic there is in the mixture, the more the material's strength will tend toward that of the plastic, which is low. These results are fully consistent with the studies in [34] [35] and work on Industrial Elaboration by Extrusion of PVC Tubes Loaded with Micronized Dura Palm Kernel Shell Powder [36].

4. Conclusion

The proposal for the use of PVC waste for the production of roof tiles should be considered by taking into account this research. From the series of tests carried out on this composite compared with other roof tiles such as those composed of cement, the recycled PVC tiles have water absorption estimations that are generally low, are lightweight, and have a long lifespan. Also, the recycled PVC tile is non-corrosive, like the corrugated iron sheets for roofing that are available in the market. Furthermore, the composition of sample 8 of the recycled PVC roof tile gives the best outcomes both physically and mechanically. This implies that the recycled PVC tile can be considered for all intents. Its qualities are moderately better, and as a result of these qualities, it can be produced in large quantities using PVC waste and river sand as an alternative for house builders. More so, when this roof tile is found to be effective, more effort will be made in adopting the product within every community, thereby reducing environmental pollution caused by waste PVC and the country's dependence on importation of roofing sheets from the western world. However, this work is just part of an investigation that can be carried out to valorize PVC waste in our communities for the production of roof covers. More research can be carried out for the application of this composite to produce poles for electrical power distribution.

Data Availability

The data used to support the findings of this study are available and can be gotten from the corresponding author upon request.

Author Contributions

Zakari Yaou: Conceptualization, funding acquisition, writing-original draft.
Laynde Tawe: Methodology, validation, formal analysis, writing-original draft.
Bernard Dadi Gaga: Methodology, validation.
Yannick Serge Evoung Nnengue: Formal analysis, writing-review & editing.
Ismael Figapka Pagore: Data curation, investigation, writing-review & editing.
Noel Konai: Supervision.
Florent Biyeme: Supervision.

Conflicts of Interest

The authors declare no conflicts of interest regarding the publication of this paper.

References

[1] Al-Sanea, S.A. (2000) Thermal Performance of Building Roof Elements. *Building and Environment*, **37**, 665-675. https://doi.org/10.1016/s0360-1323(01)00077-4

[2] Liu, Y., Yang, W.M. and Hao, M.F. (2010) Research on Mechanical Performance of Roof Tiles Made of Tire Powder and Waste Plastic. *Advanced Materials Research*, **87**, 329-332. https://doi.org/10.4028/www.scientific.net/amr.87-88.329

[3] Narayana, S. and Mathews, M.S. (2004) Behaviour of Roofing Sheet Systems under Static Uplift Loads.

[4] Chen, Y., Chen, M., Li, Y., Wang, B., Chen, S. and Xu, Z. (2016) Impact of Technological Innovation and Regulation Development on E-Waste Toxicity: A Case Study of Waste Mobile Phones. *Scientific Reports*, **8**, Article No. 7100. https://doi.org/10.1038/s41598-018-25400-0

[5] Kumar, K.S. and Stathopoulos, T. (2000) Wind Loads on Low Building Roofs: A Stochastic Perspective. *Journal of Structural Engineering*, **126**, 944-956. https://doi.org/10.1061/(asce)0733-9445(2000)126:8(944)

[6] Rajak, D.K., Pagar, D.D., Kumar, R. and Pruncu, C.I. (2019) Recent Progress of Reinforcement Materials: A Comprehensive Overview of Composite Materials. *Journal of Materials Research and Technology*, **8**, 6354-6374. https://doi.org/10.1016/j.jmrt.2019.09.068

[7] Ozerkan, N.G., Ahsan, B., Mansour, S. and Iyengar, S.R. (2014) Mechanical Performance and Durability of Treated Palm Fiber Reinforced Mortars. *International Journal of Sustainable Built Environment*, **2**, 131-142. https://doi.org/10.1016/j.ijsbe.2014.04.002

[8] Merlo, A., Lavagna, L., Suarez-Riera, D. and Pavese, M. (2020) Mechanical Properties of Mortar Containing Waste Plastic (PVC) as Aggregate Partial Replacement. *Case Studies in Construction Materials*, **13**, e00467. https://doi.org/10.1016/j.cscm.2020.e00467

[9] Davidson, M., Graunke, R., Green, A., Haelsig, H., Heinemann, L., Antony Jose, S., *et al*. (2026) Carbon Fiber-Reinforced Polymer Matrix Composites: Processing, Properties, and Applications. *Fibers*, **14**, Article 29. https://doi.org/10.3390/fib14030029

[10] Nisticò, R., Lavagna, L., Versaci, D., Ivanchenko, P. and Benzi, P. (2020) Chitosan and Its Char as Fillers in Cement-Base Composites: A Case Study. *Boletín de la Sociedad Española de Cerámica y Vidrio*, **59**, 186-192. https://doi.org/10.1016/j.bsecv.2019.10.002

[11] Suarez-Riera, D., Merlo, A., Lavagna, L., Nisticò, R. and Pavese, M. (2020) Mechanical Properties of Mortar Containing Recycled Acanthocardia Tuberculata Seashells as Aggregate Partial Replacement. *Boletín de la Sociedad Española de Cerámica y Vidrio*, **60**, 206-210. https://doi.org/10.1016/j.bsecv.2020.03.011

[12] Bolat, H. and Erkus, P. (2016) Use of Polyvinyl Chloride (PVC) Powder and Granules as Aggregate Replacement in Concrete Mixtures. *Science and Engineering of Composite Materials*, **23**, 209-216. https://doi.org/10.1515/secm-2014-0094

[13] Singh, N., Hui, D., Singh, R., Ahuja, I.P.S., Feo, L. and Fraternali, F. (2017) Recycling of Plastic Solid Waste: A State of Art Review and Future Applications. *Composites Part B: Engineering*, **115**, 409-422. https://doi.org/10.1016/j.compositesb.2016.09.013

[14] Ferrè, F., Via, A., Ausiello, G., *et al*. (2020) Sustainable Development and the Exploitation of Mineral and Energy Resources: A Review. *International Journal of Earth Science*, **91**, 723-745.

[15] Gu, L. and Ozbakkaloglu, T. (2016) Use of Recycled Plastics in Concrete: A Critical

Review. *Waste Management*, **51**, 19-42.
https://doi.org/10.1016/j.wasman.2016.03.005

[16] Nafu, Y., Gilbert, T., Albert, W., Paul, Y., Tendo, F., Saingwea, R., *et al.* (2024) Experimental Study of Physical Properties of River Sand on the Mechanical Properties of Sand/Plastic Composites for Roofing. *Composite Materials*, **8**, 44-56.
https://doi.org/10.11648/j.cm.20240802.13

[17] Kurup, A.R. and Kumar, K.S. (2017) Novel Fibrous Concrete Mixture Made from Recycled PVC Fibers from Electronic Waste. *Journal of Hazardous, Toxic, and Radioactive Waste*, **21**, 1-7. https://doi.org/10.1061/(asce)hz.2153-5515.0000338

[18] Jameel, G.S., Abdulazeez, B., Mohammed, M. and Al-Hadithi, A. (2022) Physical and Mechanical Properties of Cementitious PVC Composites. *Al-Nahrain Journal for Engineering Sciences*, **25**, 159-164. https://doi.org/10.29194/njes.25040159

[19] Jiang, L.N., Min, Y.R., Yuan, J.H., *et al.* (2026) An Empirical Study on the Thermal Environment Improvement and Energy Conservation of High-Reflective-Evaporative Composite Roofs. *Building and Environment*, **288**, Article 113949.
https://doi.org/10.1016/j.buildenv.2025.113949

[20] Basyouni, Y.A., Shokry, H., Murata, R. and Mahmoud, H. (2026) Novel Development of Affordable Composite Eco-Cool Roof Tiles from Waste Materials: An Experimental Study. *Architectural Engineering and Design Management*, 1-26.
https://doi.org/10.1080/17452007.2026.2655287

[21] Eli, L.G., Melo, A.P. and Lamberts, R. (2024) How to Improve the Thermal Performance of Buildings with One Simulation Run? The Heat Exchange Index Applied to Hot Climates. *Building and Environment*, **258**, Article 111606.
https://doi.org/10.1016/j.buildenv.2024.111606

[22] Mohammed, A.A., Mohammed, I.I. and Mohammed, S.A. (2019) Some Properties of Concrete with Plastic Aggregate Derived from Shredded PVC Sheets. *Construction and Building Materials*, **201**, 232-245.
https://doi.org/10.1016/j.conbuildmat.2018.12.145

[23] Sharma, R. and Bansal, P.P. (2016) Use of Different Forms of Waste Plastic in Concrete—A Review. *Journal of Cleaner Production*, **112**, 473-482.
https://doi.org/10.1016/j.jclepro.2015.08.042

[24] Verma, S. and Arora, S. (2015) Replacement of Natural Sand in Concrete by Polyethylene Bottles. *International Restrictive Journal of Engineering and Technology*, **2**, 120-124.

[25] Haghighatnejad, N., Mousavi, S.Y., Khaleghi, S.J., Tabarsa, A. and Yousefi, S. (2016) Properties of Recycled PVC Aggregate Concrete under Different Curing Conditions. *Construction and Building Materials*, **126**, 943-950.
https://doi.org/10.1016/j.conbuildmat.2016.09.047

[26] Bisong, M.S., Mikhailov, V.E., Lepov, V.V. and Makharova, S.N. (2019) Microstructure Influence on Crack Resistance of Steels Welded Structures Operated in an Extremely Cold Environment. *Procedia Structural Integrity*, **20**, 37-41.
https://doi.org/10.1016/j.prostr.2019.12.112

[27] Mohammed, A.A. (2017) Flexural Behaviour and Analysis of Reinforced Concrete Beams Made of Recycled PET Waste Concrete. *Construction and Building Materials*, **155**, 593-604. https://doi.org/10.1016/j.conbuildmat.2017.08.096

[28] Chandni, T.J. and Anand, K.B. (2018) Utilization of Recycled Waste as Filler in Foam Concrete. *Journal of Building Engineering*, **19**, 154-160.
https://doi.org/10.1016/j.jobe.2018.04.032

[29] Pascoe, R.D. and O'Connell, B. (2003) Development of a Method for Separation of

PVC and PET Using Flame Treatment and Flotation. *Minerals Engineering*, **16**, 1205-1212. https://doi.org/10.1016/s0892-6875(03)00171-7

[30] Stoltz, G., Gourc, J. and Oxarango, L. (2010) Characterisation of the Physico-Mechanical Parameters of MSW. *Waste Management*, **30**, 1439-1449. https://doi.org/10.1016/j.wasman.2010.03.016

[31] Jassim, A.K. (2017) Recycling of Polyethylene Waste to Produce Plastic Cement. *Procedia Manufacturing*, **8**, 635-642. https://doi.org/10.1016/j.promfg.2017.02.081

[32] Bamigboye, G.O., Ngene, B.U., Ademola, D. and Jolayemi, J.K. (2019) Experimental Study on the Use of Waste Polyethylene Terephthalate (PET) and River Sand in Roof Tile Production. *Journal of Physics*: *Conference Series*, **1378**, Article 042105. https://doi.org/10.1088/1742-6596/1378/4/042105

[33] Seghiri, M., Boutoutaou, D., Kriker, A. and Hachani, M.I. (2017) The Possibility of Making a Composite Material from Waste Plastic. *Energy Procedia*, **119**, 163-169. https://doi.org/10.1016/j.egypro.2017.07.065

[34] Guendouz, M., Debieb, F., Boukendakdji, O., Kadri, E.H., *et al*. (2016) Use of Plastic Waste in Sand Concrete. *Journal of Materials and Environmental Science*, **7**, 382-389.

[35] Ghernouti, Y. and Rabehi, B. (2011) Béton à base des granulats de déchets des sacs en plastique renforcé de fibres métalliques. NVACO2: Séminaire international, innovation et valorisation en génie civil et matériaux de construction, 7p.

[36] Djomi, R., Fokam, C.M., Biyeme, F., Mveh, C.M., Olembé, R., Ntede, H., *et al*. (2021) Industrial Elaboration by Extrusion of PVC Tubes Loaded with Micronized Dura Palm Kernel Shell Powder. *Journal of Materials Science and Chemical Engineering*, **9**, 41-69. https://doi.org/10.4236/msce.2021.910004